SLAC–PUB–10694
August 2004

Generation of GW-level, sub-Angstrom Radiation in the LCLS using a Second-Harmonic Radiator *

Z. Huang †

Stanford Linear Accelerator Center, Menlo Park, CA 94025

S. Reiche

UCLA, Los Angeles, CA 90095

Abstract

Electron beams are strongly microbunched near the high-gain free-electron laser (FEL) saturation with a rich harmonic content in the beam current. While the coherent harmonic emission is possible in a planar undulator, the third-harmonic radiation typically dominates with about 1% of the fundamental power at saturation. In this paper, we discuss the second-harmonic radiation in the Linac Coherent Light Source. We show that by a suitable design of an second-stage undulator with its fundamental frequency tuned to the second harmonic of the first undulator, coherent second-harmonic radiation much more intense than the third-harmonic is emitted. Numerical simulations predict that GW-level, sub-Angstrom x-ray pulses can be generated in a relatively short second-harmonic radiator.

Presented at the 26th International Free-Electron Laser Conference and 11th FEL User Workshop (August 29 - September 3, 2004, Trieste, Italy)

*Work supported by Department of Energy contract DE–AC02–76SF00515.
†Email: zrh@slac.stanford.edu

Generation of GW-level, sub-Angstrom Radiation in the LCLS using a Second-Harmonic Radiator *

Z. Huang†, SLAC, Stanford, CA 94309, USA
S. Reiche, UCLA, Los Angeles, CA 90095, USA

Abstract

Electron beams are strongly microbunched near the high-gain free-electron laser (FEL) saturation with a rich harmonic content in the beam current. While the coherent harmonic emission is possible in a planar undulator, the third-harmonic radiation typically dominates with about 1% of the fundamental power at saturation. In this paper, we discuss the second-harmonic radiation in the Linac Coherent Light Source. We show that by a suitable design of an second-stage undulator with its fundamental frequency tuned to the second harmonic of the first undulator, coherent second-harmonic radiation much more intense than the third-harmonic is emitted. Numerical simulations predict that GW-level, sub-Angstrom x-ray pulses can be generated in a relatively short second-harmonic radiator.

INTRODUCTION

In a single-pass, high-gain free-electron laser (FEL) strong bunching at the fundamental wavelength can drive substantial nonlinear harmonic bunching [1]. For a planar undulator, third-harmonic radiation can typically reach 1% of the fundamental power level at saturation [2, 3]. While comparable second-harmonic power has been observed at the VISA [4] and the LEUTL [5] FELs and is in agreement with the theoretical expectations [6], the second-harmonic content is in general much smaller than 1% of the fundamental at very high-energy FELs such as the Linac Coherent Light Source (LCLS) [7]. To further increase the harmonic emission, a second undulator with its fundamental frequency tuned to a harmonic number of the first undulator may be used [8, 9, 10]. A major concern of this method is the effectiveness of the second undulator due to the increased beam energy spread induced by the nonlinear FEL interaction in the first undulator. Another harmonic generation method for a self-amplified spontaneous emission (SASE) FEL [11], similar to the high-gain harmonic generation (HGHG) scheme for seeded FELs [12], proposes to operate the first undulator in the linear regime for energy modulation and to use a dispersion section for nonlinear harmonic bunching. The relatively cold beam can then be sent into a second undulator for effective harmonic generation.

The shortest-wavelength x-ray for the LCLS fundamental radiation is 1.5 Å. While there is a great interest in reaching shorter x-ray wavelengths such as the 0.86-Å ^{57}Fe Mössbauer spectroscopy, generation and saturation of the FEL fundamental radiation at 1 Å or below is extremely difficult with the present state of the art electron beams (see, e.g., Ref. [13]). In this paper, we show that the second-harmonic radiation in the main LCLS undulator is very small and can be significantly enhanced by a second-harmonic radiator in order to expand the wavelength range and scientific capabilities of the facility. Since the electron beam quality at x-ray wavelengths is usually limited by the beam emittance rather than by the energy spread, operating the first undulator at saturation does not severely affect the performance of the second harmonic radiator. Instead, we find that by optimizing the focusing strength in the second-harmonic radiator and by applying the appropriate undulator taper, we can effectively extract more than 10% of the fundamental power in a relatively short undulator, which can then operate parasitically to the first undulator. Fully three-dimensional, time-dependent FEL simulation code GENESIS [14] is used to predict the performance of the second-harmonic radiator.

SECOND-HARMONIC CONTENT IN THE MAIN LCLS UNDULATOR

The LCLS uses the last one-third of the SLAC linac (about $\gamma mc^2 \approx 14$ GeV) to drive an x-ray SASE FEL at the fundamental wavelength $\lambda_1 = 1.5$ Å to reach a saturation power $P_1 \approx 10$ GW in a 100-m undulator. It is expected that the third-harmonic power can reach 100 MW near saturation. Although the second-harmonic bunching is higher than the third-harmonic bunching due to the nonlinear harmonic interaction, only odd harmonics are emitted in the forward direction. Even harmonics radiation can be emitted off-axis for a single electron and hence are present for a beam with a finite transverse extension [15]. In addition, even-harmonic emissions may be enhanced for a misaligned beam trajectory [16]. Before investigating the performance of the second-harmonic radiator, we estimate in this section the second-harmonic content in the main LCLS undulator due to both of these two effects.

The electron motion in the undulator consists of a fast wiggling oscillation and a slow betatron trajectory. Let us write the transverse velocities as $v_x = c[K/\gamma \cos(k_u z) + x']$ and $v_y = cy'$, where K is the undulator parameter, $\lambda_u = 2\pi/k_u$ is the undulator period, x' and y' are the transverse angles of the slow trajectory, and z is the undulator

* Work supported by the U.S. Department of Energy contract DE-AC02-76SF00515.

† zrh@slac.stanford.edu

distance. The longitudinal velocity is

$$\frac{dz}{dt} = v_z = \sqrt{v^2 - v_x^2 - v_y^2} = c\left[1 - \frac{1}{2\gamma^2} - \frac{K^2}{4\gamma^2} - \frac{K^2}{4\gamma^2}\cos(2k_u z) - \frac{Kx'}{\gamma}\cos(k_u z) - \frac{x'^2 + y'^2}{2}\right]. \quad (1)$$

It is convenient to treat z as the independent variable, and regard t as the electron arrival time at the undulator distance z. Integrating Eq. (1) yields

$$ct = ct^* + \frac{K^2}{8k_u\gamma^2}\sin(2k_u z) + \frac{Kx'}{k_u\gamma}\sin(k_u z),$$
$$ct^* = \left(1 + \frac{1 + K^2/2}{2\gamma^2} + \frac{x'^2 + y'^2}{2}\right) z, \quad (2)$$

where $(x'^2 + y'^2)$ is taken to be approximately constant after averaging over one FODO cell [17]. Thus, the average longitudinal motion ct^* is accompanied by a longitudinal oscillation at twice of the transverse wiggling frequency ck_u, as well as another longitudinal oscillation at the wiggling frequency due to the coupling to the horizontal orbit. We can change the time variable t to the ponderomotive phase θ:

$$\theta(z) = (k_u + k_1)z - ck_1 t^* \quad (3)$$
$$= (k_u + k_1)z - ck_1 t + \xi\sin(2k_u z) + \frac{8x'\xi}{K/\gamma}\sin(k_u z),$$

where $k_1 = 2\pi/\lambda_1 = 2\gamma^2 k_u/(1 + K^2/2)$ is the fundamental wavenumber and $\xi = K^2/(4+2K^2)$. Inserting this expression into the paraxial wave equation (e.g., Eq. (2) of Ref. [6]) and expanding the exponent for $8\gamma x'\xi/K \ll 1$, the n^{th} harmonic field E_n ($n = 1, 2, ...$) is given by

$$\left(\frac{\partial}{\partial z} + \frac{\nabla_\perp^2}{2ink_1}\right)E_n \approx -\frac{ecKZ_0}{\gamma\lambda_1}\int_{-\infty}^{\infty} d\theta e^{-in\theta} \times e^{ink_u z + in\xi\sin(2k_u z)}\cos(k_u z)\sum_{j=1}^{N_e}\delta(y - y_j)\,\delta(\theta - \theta_j) \times \left[\delta(x - x_j) + in\xi\frac{8x'_j}{K/\gamma}\sin(k_u z)\delta(x - x_j) - \frac{K}{\gamma k_u}\sin(k_u z)\delta'(x - x_j)\right], \quad (4)$$

where $\nabla_\perp^2$ is the transverse Laplace, $Z_0 = 377\ \Omega$ is the vacuum impedance, $\delta'(x) = d\delta(x)/dx$, and the sum is over N_e electrons.

Since both the FEL interaction and the betatron motion occur on a length scale much longer than the fast wiggling motion, we can average the current source (the right hand side) of Eq. (4) over the wiggling motion. The first term in the square bracket contributes to odd-harmonic radiation in the forward direction. After summing over all electrons for the second term in the square bracket, we obtain even-harmonic radiation due to trajectory errors with the coupling strength $8n\gamma x'_c\xi/K$, where x'_c is the trajectory angle of the beam centroid motion. Summing over all electrons for the last term of the square bracket yields even-harmonic emissions due to a finite beam size with the coupling strength $K/(\gamma k_u\sigma_x)$) [6], where σ_x is the rms transverse size of the electron beam. Using a bunching parameter $b_n = |\sum_{j=1}^{N_e} e^{-in\theta_j}|/N_e$ to characterize the current source at the n^{th} harmonic, we can estimate the second-harmonic power P_2 due to a finite beam size as

$$P_2 \approx P_1\left(\frac{K}{\gamma k_u\sigma_x}\right)^2\left(\frac{[\text{JJ}]_2}{[\text{JJ}]}\right)^2\frac{b_2^2}{b_1^2}, \quad (5)$$

where the Bessel function factors are $[\text{JJ}] = [J_0(\xi) - J_1(\xi)]$ and $[\text{JJ}]_2 = [J_0(2\xi) - J_2(2\xi)]/2 = J'_1(2\xi)$. Similarly, we can estimate the second-harmonic emission due to trajectory errors as

$$P_2 \approx P_1\left(\frac{8\gamma K\langle(x'_c)^2\rangle^{1/2}}{2 + K^2}\right)^2\left(\frac{[\text{JJ}]_2}{[\text{JJ}]}\right)^2\frac{b_2^2}{b_1^2}, \quad (6)$$

where $\langle(x'_c)^2\rangle^{1/2}$ is the rms angle of the beam trajectory.

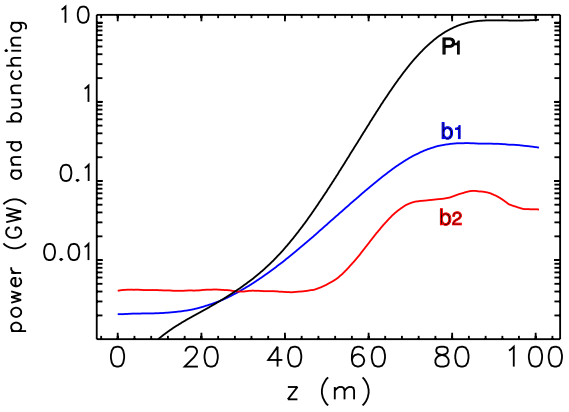

Figure 1: Fundamental radiation power (black) and bunching (blue), second-harmonic bunching (red) along the main LCLS undulator.

The evolution of the fundamental and the harmonic bunching is determined by the nonlinear interaction of the fundamental radiation field with the electron beam. Figure 1 shows GENESIS simulation of the fundamental and the second-harmonic bunching for an average beta function $\langle\beta\rangle = 30$ m in the LCLS undulator. The electron beam is assumed to have a normalized transverse emittance $\gamma\epsilon = 1.2\ \mu$m, a peak current $I_0 = 3.4$ kA, and an initial rms relative energy spread $\sigma_{\delta 0} = 1 \times 10^{-4}$. For simplicity, no drift spaces between undulator sections are included in our simulations. At the FEL saturation (around $z = 86$ m), we have $|b_1| \approx 0.30$ and $|b_2| \approx 0.075$. Taking $K = 3.7$ and $\lambda_u = 3$ cm, we obtain from Eq. (5) that $P_2 \approx 50$ kW for a perfect trajectory. For BPMs that have a resolution of about 2-μm and are separated by about 4 m, the tolerable rms trajectory misalignment angle is $\langle(x'_0)^2\rangle^{1/2} \approx 2/4 = 0.5\ \mu$rad [18]. Assuming the FEL still

reaches saturation in the 100-m undulator, Eq. (6) yields 110 kW additional second-harmonic power due to the imperfect trajectory, still three orders of magnitude smaller than the expected third-harmonic power.

COHERENT HARMONIC GENERATION IN THE SECOND-HARMONIC RADIATOR

Since there is substantial second-harmonic bunching at the FEL saturation, it should be possible to significantly increase the second-harmonic radiation by using a second-stage undulator with its resonant wavelength tuned to the second-harmonic wavelength (i.e., $\lambda_2 = 0.75$ Å) of the LCLS. In this section, we study and optimize the performance of such a second-harmonic radiator. Table 1 lists the parameters for a planar Nd-Fe-B undulator that is resonant at 0.75 Å. The undulator gap $g = 5$ mm and the peak magnetic field B_0 are determined by Halbach's formula [19]. Since the field quality tolerance of the second-harmonic radiator is expected to be more relaxed than the first undulator, a helical undulator (with a wider gap) may be used to generate circularly-polarized second-harmonic radiation.

Table 1: Parameters for the LCLS second-harmonic radiator.

Parameter	symbol	value	unit
undulator period	λ_{u2}	2.38	cm
undulator gap	g	5	mm
peak magnetic field	B_0	1.26	Tesla
undulator parameter	K_2	2.81	
resonant wavelength	λ_2	0.75	Å
undulator length	L_{u2}	43	m
total linear taper	$\Delta K_2/K_2$	0.25	%
average beta function	$\langle\beta_2\rangle$	15	m

For a pre-bunched beam entering the second-harmonic radiator, the coherent radiation power is given by [20]

$$P_2 = \frac{I_0^2 Z_0}{8\gamma^2}\frac{K_2^2[\mathrm{JJ}]^2}{4\pi\sigma_x^2}\left(\int_0^{L_{u2}} b_2(z)dz\right)^2, \qquad (7)$$

where the Bessel function factor [JJ] is now evaluated for the new undulator parameter K_2. We see that a smaller transverse beam size can generate more coherent radiation, but the increased angular spread also leads to a larger spread in ponderomotive phase that degrades the bunching. The phase spread due to the emittance can be estimated from Eqs. (2) and (3) for the second-harmonic phase θ_2:

$$\left\langle \frac{d\theta_2}{dz} \right\rangle = \frac{2\pi}{\lambda_2}\sigma_{x'}^2 = \frac{2\pi}{\lambda_2}\frac{\epsilon}{\langle\beta_2\rangle}. \qquad (8)$$

For the FEL that reaches saturation in the first undulator, the micro-bunched beam has a rms relative energy spread $\sigma_{\delta f} \approx \rho \approx 4.5\times10^{-4}$, where ρ is the FEL parameter [21].

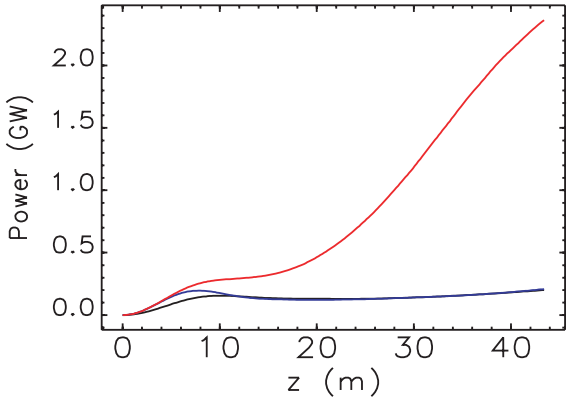

Figure 2: Radiation power in the second-harmonic radiator for (a) 15-m average beta, 0.25% linearly tapered undulator (red), (b) 15-m average beta, uniform undulator (blue) and (c) 30-m average beta, uniform undulator (black).

The resulting second-harmonic phase spread is

$$\left\langle \frac{d\theta_2}{dz} \right\rangle = \frac{4\pi}{\lambda_{u2}}\sigma_{\delta f} \approx \frac{4\pi}{\lambda_{u2}}\rho. \qquad (9)$$

The optimal focusing strength is obtained when the right hand side of both Eqs. (8) and (9) are equal. Thus, an average beta function $\langle\beta_2\rangle \approx \epsilon\lambda_{u2}/(2\rho\lambda_2) \approx 15$ m would generate the most coherent harmonic power without degrading the bunching beyond the level caused by the energy spread. Note that this value of the average beta function is about a factor of 2 smaller than the average beta function in the LCLS main undulator.

To simulate harmonic generation, GENESIS has been upgraded to allow for up-conversion of its internal particle distribution to higher harmonics. The particle phases are converted by $\theta_n = n\theta$, filling n successive slices to keep the spectral resolution of the simulation constant. It also requires a change in the shot noise algorithm to provide the correct bunching statistics on all harmonics supported by the simulation, and follows closely the method of harmonic decomposition of the fluctuation in the particle phase [22]. For the second-harmonic generation, the electron distribution is extracted at a post-saturation distance $z \approx 90$ m of the first undulator (with $b_2 \approx 0.06$ instead of the maximum value 0.075). As seen in Fig. 1, the second-harmonic bunching is somewhat reduced from the maximum value after saturation. If necessary, this reduction may be minimized by a slight increase of the initial energy spread with a designated energy-spread heater in the LCLS [23] to allow the FEL saturation at the end of the first undulator. The electron transverse phase space is assumed to be properly matched into the second undulator.

At this optimal focusing strength, the rapid build-up of coherent power in the second-harmonic radiator enables tapering the undulator parameter K_2 in order to trap sufficient electrons for effective harmonic generation. For simplicity, we consider here only a linear taper that starts at the beginning of the undulator. The taper strength is

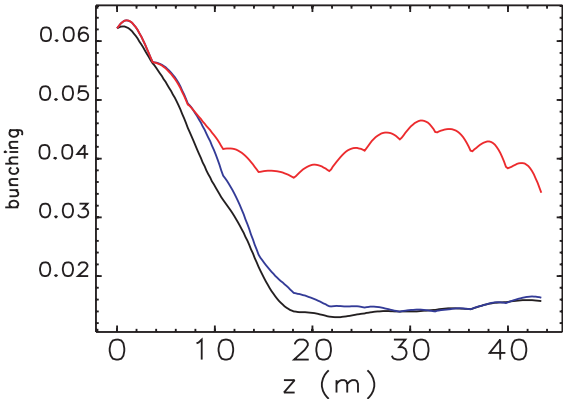

Figure 3: Bunching parameter in the second-harmonic radiator for (a) 15-m average beta, 0.25% linearly tapered undulator (red), (b) 15-m average beta, uniform undulator (blue) and (c) 30-m average beta, uniform undulator (black).

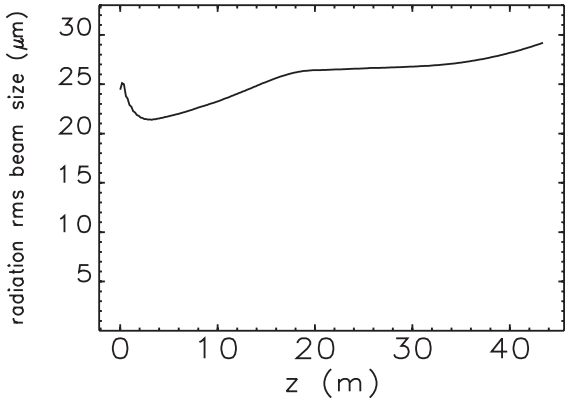

Figure 4: RMS beam size of the 0.75-Å radiation along the second-harmonic radiator.

then varied to maximize the output power. Figure 2 shows SASE simulations of both tapered and uniform undulators at $\langle\beta_2\rangle = 15$ m. An 43-m tapered undulator with a taper strength $\Delta K_2/K_2 = 0.25$ % generates more than 2 GW output power at 0.75 Å, which is about one order of magnitude larger than that from the uniform undulator. Examination of Fig. 3 indicates the effectiveness of the undulator taper in maintaining the second-harmonic bunching against the phase spread from both the emittance and the energy spread, while the bunching parameter drops almost independent of the focusing strength for a uniform undulator. Figure 2 also shows that a larger beam size in the undulator (with $\langle\beta_2\rangle = 30$ m) generates less coherent radiation initially. Hence the undulator taper may not be as effective.

Finally, Fig. 4 shows that the radiation rms beam size along the second-harmonic radiator follows closely to the rms electron beam size ($\sigma_x = 26$ μm), indicating a nearly diffraction-limited radiation at 0.75 Å. The relative rms spectrum bandwidth of the 0.75-Å radiation is about 0.05%, similar to the bandwidth of the saturated fundamental radiation at 1.5 Å in the first undulator. These x-ray pulses from both undulators are naturally synchronized as they are generated by the same electron beam.

CONCLUSIONS

Given that the LCLS reaches saturation in the planned 100-m undulator, the significant second-harmonic bunching can still be very useful in generating high-power, shorter-wavelength coherent radiation which is otherwise difficult to obtain with the current electron beam technology. The analysis and simulations presented in this paper show that an second-harmonic radiator operating parasitically to the main LCLS undulator can effectively produce GW-level, sub-Angstrom x-rays for scientific applications.

We thank P. Emma, J. Hastings, and K.-J. Kim for useful discussions.

REFERENCES

[1] R. Bonifacio, L. De Salvo, and P. Pierini, Nucl. Instr. Meth. A **293**, 627 (1990).

[2] H.P. Freund, S.G. Biedron, and S.V. Milton, IEEE J. Quantum Electron. **QE-36**, 275 (2000); Nucl. Instr. Meth. A **445**, 53 (2000).

[3] Z. Huang and K.-J. Kim, Phys. Rev. E, **62**, 7259 (2000).

[4] A. Tremaine *et al.*, Phys. Rev. Lett. **88**, 204801 (2002).

[5] S. Biedron *et al.*, Nucl. Instr. Meth. A **483**, 94 (2002).

[6] Z. Huang and K.-J. Kim, Nucl. Instr. Meth. A **475**, 112 (2001).

[7] Linac Coherent Light Source Conceptual Design Report, SLAC-R-593, 2002.

[8] R. Bonifacio *et al.*, Nucl. Instr. Meth. A **296**, 787 (1990).

[9] W. Fawley *et al.*, in *Proceedings of the 1995 Particle Accelerator Conference*, 219 (IEEE, Piscataway, NJ,1995).

[10] F. Ciocci *et al.*, IEEE J. Quantum Electron. **QE-31**, 1242 (1995);.

[11] J. Feldhaus *et al.*, Nucl. Instr. Meth. A **528**, 471 (2004).

[12] L.H. Yu, Phys. Rev. A **44**, 5178 (1991).

[13] M. Cornacchia, J. Synchrotron Rad. **11**, 227 (2004).

[14] S. Reiche, Nucl. Instrum. Methods Phys. Res. A **429**, 243 (1999).

[15] M.J. Schmitt and C.J. Elliott, Phys. Rev. A **34**, 4843 (1986).

[16] W.B. Colson, G. Dattoli, and F. Ciocci, Phys. Rev. A **31**, 828 (1985).

[17] S. Reiche, Nucl. Instrum. Methods Phys. Res. A **445**, 90 (2000).

[18] P. Emma, private communication.

[19] K. Halbach, J. Phys. (Paris) Colloq. **44**, C1-211 (1983).

[20] L.H. Yu and J. Wu, Nucl. Instrum. Methods Phys. Res. A **483**, 493 (2002).

[21] R. Bonifacio, C. Pellegrini, and L.M. Narducci, Opt. Comm. **50**, 373 (1984).

[22] W. Fawley, Phys. Rev. ST Accel. Beams 5, 070701 (2002).

[23] Z. Huang *et al.*, Phys. Rev. ST Accel. Beams **7**, 074401 (2004).